

Magnetic characterization of PdNi contact electrodes

D. Steininger,^{1, a)} A. K. Hüttel,¹ M. Ziola,¹ M. Kiessling,¹ M. Sperl,¹ G. Bayreuther,¹ and Ch. Strunk¹

Institute for Experimental and Applied Physics, University of Regensburg, Universitätsstr. 31, D-93053 Regensburg, Germany

We investigate submicron ferromagnetic PdNi thin-film strips intended as contact electrodes to carbon nanotube-based spintronic devices. The strips are studied for their magnetic properties with respect to magnetic anisotropy and micromagnetic structure, depending on temperature and aspect ratio. Magnetic hysteresis measurements of Pd_{0.3}Ni_{0.7} using SQUID magnetometry are performed on arrays containing strips of various width, and point towards a magnetically easy axis transversal to the strip direction. For further investigation of spontaneous magnetization, the anisotropic magnetoresistance is measured on individual Pd_{0.3}Ni_{0.7} contact strips, and magnetic force microscopy is performed. Both confirm independently this magnetic structure of the electrodes.

Carbon nanotubes (CNTs) have become a frequently used material for spin dependent transport experiments within the past years. Due to spin lifetimes of several nanoseconds,^{1,2} CNTs provide excellent conditions for this kind of investigation.^{3–5} Spin injection requires ferromagnetic contact electrodes to the CNT which provide both spin polarization and a transparent electric contact. As palladium is known for its high contact transparency to CNTs,^{3,5–8} an alloy of palladium with nickel as ferromagnetic material was chosen for this study. The electronic properties of pure palladium^{9,10} and especially the formation of giant magnetic moments in dilute alloys with small amounts of ferromagnetic elements have been well studied for both bulk material and thin films, with respect to Curie points and critical alloy concentrations for the onset of ferromagnetism.^{11–16}

Objective of this work is the investigation of thin film Pd_{0.3}Ni_{0.7} high aspect ratio shapes, particularly with regard to their suitability as ferromagnetic contact electrodes for CNT devices. While a seemingly similar alloy Pd_{1–x}Fe_x has been studied in much detail with respect to its magnetic contact properties,^{4,11,12,17,18} these findings are not transferable to Pd_{1–x}Ni_x due to the significantly different crystal properties of nickel and iron and the differing ferromagnet concentrations in the experiments.¹⁹

We use Pd_{0.3}Ni_{0.7} strips at widths of 250 nm — 1500 nm, maintaining a constant length of 5 μ m and metal film thickness of 50 nm. All samples were fabricated on a boron doped, p++ type Si substrate with thermally grown SiO₂ surface oxide, and structured via electron beam lithography and lift-off process using a polymethyl methacrylate two layer resist. The deposition of the thin films was done by electron beam evaporation from pre-mixed bulk material in an UHV evaporation system with a base pressure of 4×10^{-8} mbar. Figure 1 displays such a strip pattern, in this particular case with leads attached in a second lithography step for magnetoresistance measurements. It also introduces the characteristic directions for all the magnetic field orientations used in this manuscript, i.e., perpendicular (P),

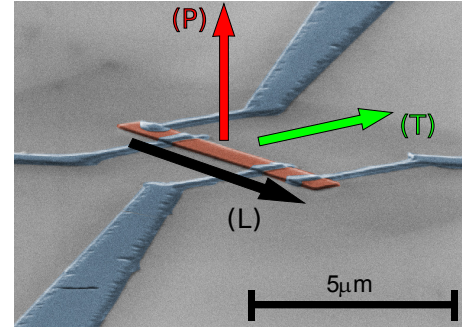


FIG. 1. (Color online) Scanning electron microscopy (SEM) image of a contacted Pd_{0.3}Ni_{0.7} strip (colorized in red). The four contact leads (colorized blue) were evaporated in a second step from pure palladium. They provide the possibility to perform four terminal resistance measurements. The arrows indicate the three tested orientations of the external magnetic field relative to the strip, namely black (L): longitudinal, red (P): perpendicular, and green (T): transverse.

transverse (T), and longitudinal (L) with respect to the Pd_{0.3}Ni_{0.7} strip.

Superconducting quantum interference device (SQUID) magnetization measurements using a commercial magnetometer have been used to characterize the averaged magnetic hysteresis of arrays containing 1.3×10^6 non-contacted, electrically isolated thin film strips. They reveal the switching characteristics for different strip widths at various temperatures and orientations of the external magnetic field. Fig. 2 displays the magnetization curves of an array of 250 nm wide strips. The total magnetic moment of the sample at $T = 300$ K is $M_{\text{tot}} = 3.7 \times 10^{-5}$ Gcm³ (see Fig. 2(a)), from which an average magnetic moment of $\bar{\mu} = 0.583\mu_B$ per alloy atom can be calculated. This value is comparable to previous results¹¹ for bulk Pd_{0.3}Ni_{0.7}. Figures 2(a-b) show overview plots over the entire hysteresis loop in a transverse (T) and longitudinal (L) external field at $T = 300$ K and $T = 2$ K, while Figures 2(c-d) zoom in onto the range $-0.4 \text{ T} \leq \mu_0 H \leq 0.4 \text{ T}$.

As can be seen in Fig. 2(b), the sample requires an external magnetic field of $\mu_0 |H| \geq 2 \text{ T}$ to reach magnetic saturation at $T = 2 \text{ K}$. This behaviour may be explained

^{a)} Electronic mail: daniel.steininger@physik.uni-r.de

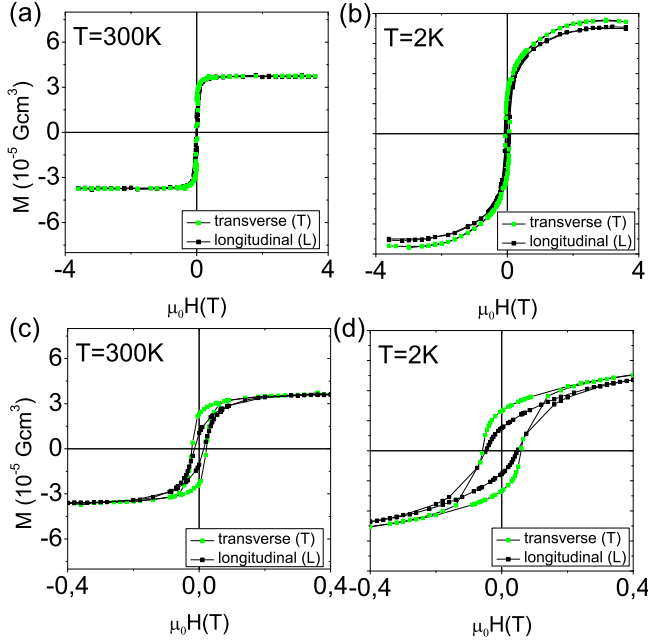


FIG. 2. (Color online) SQUID magnetization measurements on an array containing 1.3×10^6 strips of 250 nm width and $5 \mu\text{m}$ length. The array was measured in an external field of $\mu_0 |H| \leq 3.6 \text{ T}$ in both transverse (T, green) and longitudinal (L, black) direction (see also Fig. 1) at $T = 300 \text{ K}$ (a,c) and $T = 2 \text{ K}$ (b,d). The upper panels (a,b) show the full field range of the hysteresis loop while the lower panels (c,d) zoom into the range $-0.4 \text{ T} \leq \mu_0 H \leq 0.4 \text{ T}$.

by paramagnetic contributions of the highly boron-doped Si substrate which vanish at room temperature.²⁰ In Fig. 2(c-d), showing the external field range $-0.4 \text{ T} \leq \mu_0 H \leq 0.4 \text{ T}$, the influence of the magnetic field orientation on the saturation field becomes visible. Saturation is reached at lower external fields for the transverse orientation of external magnetic field. Also the remanent magnetization in transverse direction is significantly higher than in longitudinal orientation. These observations indicate an initially unexpected magnetically easy axis along this direction (T).

To obtain further information on the direction of spontaneous magnetization and the switching behaviour of single contact electrodes, the anisotropic magnetoresistance (AMR) of individually contacted $\text{Pd}_{0.3}\text{Ni}_{0.7}$ strips was measured. As with the samples for the SQUID measurements, the strips were fabricated via electron beam lithography and lift-off process on identical Si/SiO₂ substrate material. The non-magnetic palladium leads (see Fig. 1) were deposited using a second electron beam lithography and evaporation step. The resistance of a ferromagnetic strip is generally higher when the current through the strip is aligned parallel to the magnetization vector of the structure ($\vec{J} \parallel \vec{M}$) than in the perpendicular case ($\vec{J} \perp \vec{M}$).^{21,22} Transport measurements were performed at $T = 4.2 \text{ K}$, applying a maximum external

magnetic field of $\mu_0 H_{\text{max}} = \pm 925 \text{ mT}$ successively in different orientations relative to the strip. The resistance measurement itself was carried out using a four-terminal setup and lock-in technique.

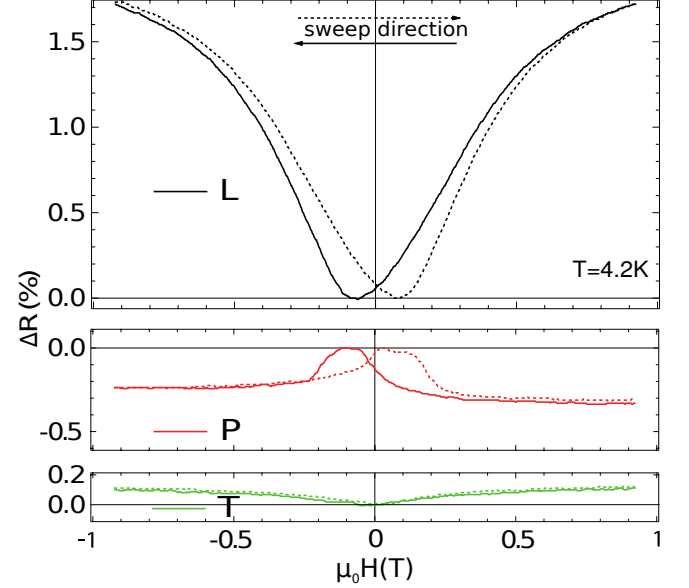


FIG. 3. (Color online) Anisotropic magnetoresistance $\Delta R = (R(\mu_0 H) - R_{\text{max}})/R_{\text{max}}$ of an individually contacted, 500 nm wide $\text{Pd}_{0.3}\text{Ni}_{0.7}$ strip. The three panels represent the relative orientation of the magnetic field according to Fig. 1, i.e. longitudinal (L, black), perpendicular (P, red) and transverse (T, green). The dashed traces show the magnetic field up-sweep, while the continuous traces show the down-sweep measurement. All three panels have identical scaling of both axes.

Fig. 3 shows the relative change of resistance in dependence on the external magnetic field $\mu_0 H$, $\Delta R = (R(\mu_0 H) - R_{\text{max}})/R_{\text{max}}$, for a strip width of 500 nm. The three panels correspond to the three field orientations as sketched in Fig. 1. The largest increase of resistance occurs when applying the field in longitudinal (L) direction. This means that a large part of the magnetization was oriented away from this direction and had to be aligned parallel to the strip by the external magnetic field. In perpendicular (P) direction we observe a decrease of the resistance. Assuming an out of plane tilt angle of the magnetization vector, this is then indeed consistent with lower resistance for a current perpendicular to the magnetization. In transverse (T) direction the minimal change of resistance appears. As result we can conjecture that the spontaneous magnetization of the strips is oriented mainly transverse to the strips' long axis. The small amount of change in resistance in a magnetic field along the transverse (T) direction means that the majority of magnetic moments already was aligned in this direction before the field was applied. As expected, the minima respectively maxima of the magnetoresistance curves show hysteretic behaviour and are mirrored according to the sweep direction of the external field.

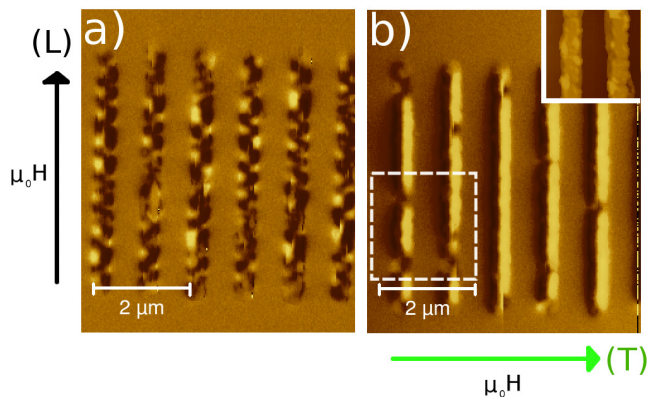


FIG. 4. (Color online) Magnetic force microscopy (MFM) images of the remanent magnetization of an ensemble of $\text{Pd}_{0.3}\text{Ni}_{0.7}$ strips. Before recording the image, the strips have been magnetized along the directions indicated by the arrows, i.e. (a) in longitudinal (L), and (b) in transverse (T) direction. The inset in (b) shows the surface topography of the region in the white dashed square

Finally, magnetic force microscopy (MFM) on a strip array directly reveals the remanent micromagnetic configuration within narrow strips (width 250nm) of $\text{Pd}_{0.3}\text{Ni}_{0.7}$. Fig. 4 displays magnetic force microscopy (MFM) images of an ensemble of contact strips. The MFM pictures were taken at room temperature and zero external magnetic field; the scanning direction was longitudinal to the strips (L). Prior to imaging, the sample was magnetized along the longitudinal (L) (Fig. 4(a)) or transverse (T) direction (Fig. 4(b)) by an external field of $\mu_0 H = 2\text{ T}$ to ensure magnetic saturation.

The pattern in Fig. 4(a), where the sample was previously magnetized in longitudinal (L) direction features alternating domain alignment along the transverse (T) direction. This is consistent with a spontaneous magnetization in transverse (T) axis, as inferred from the SQUID and AMR measurements; the longitudinal (L) remanence detected in Fig. 2(c,d) can arise if the magnetization in adjacent domains is not exactly antiparallel, summing up to a finite longitudinal (L) component, or the domain splitting is not perfectly symmetric due to a small misalignment of the saturating field relative to the magnetically hard axis. In Fig. 4(b), after magnetizing in (T) direction the magnetization structure in this direction is considerably more stable. The strips feature large domains with transverse (T) magnetization direction. The remaining disintegration into domains in certain areas may be caused by, e.g., edge roughness of the strips, supported by thermal activated processes at room temperature: in the inset of Fig. 4(b), showing the surface topography of the region marked by a white square in the MFM picture, several magnetic features re-appear as height profile irregularities. Altogether, MFM imaging again confirms the findings of an easy axis along the transverse (T) direction.

A possible explanation for the transverse magnetic easy axis is the effect of inverse magnetostriction.²³ While many mechanisms can contribute local stress during fabrication of the strips, it is already instructive to look at the highly different thermal expansion coefficients α of the thin film metal ($\alpha_{\text{Pd}} \approx 11.8 \times 10^{-6} \text{ K}^{-1}$, $\alpha_{\text{Ni}} \approx 13.4 \times 10^{-6} \text{ K}^{-1}$) and the substrate material used in this study ($\alpha_{\text{Si}} \approx 2.6 \times 10^{-6} \text{ K}^{-1}$). Considering a temperature higher than room temperature during the thin film evaporation process of PdNi, tensile stress is imprinted on the metal layer when the sample is cooled down. At the edges of the strips, this stress can relax. If the strip is sufficiently narrow the relaxation of transversal stress takes place across the entire strip. Assuming a similar behaviour of $\text{Pd}_{0.3}\text{Ni}_{0.7}$ and pure nickel (due to the high amount of nickel in our alloy and the same crystal structure (fcc) of both elements), the magnetic moments in the strip then align orthogonal to the remaining longitudinal stress, i.e. in the transversal (T) direction, as the magnetostriction coefficient of nickel is negative for both (100) and (111) direction.²³

As a conclusion, our work confirms in all aspects that the magnetic preferential direction of high aspect ratio $\text{Pd}_{0.3}\text{Ni}_{0.7}$ thin film contact strips behaves contrary to previous investigated $\text{Pd}_x\text{Fe}_{1-x}$ contacts.^{4,17} The strips feature a magnetically easy axis transverse to the strip orientation. This can be explained by the effect of magneto-elastic coupling. It dominates other mechanisms as e.g. shape anisotropy, which would favour a magnetically easy axis longitudinal to the strip orientation. For application of our investigated contact strips in CNT based spin devices it is therefore recommended to apply external magnetic fields in transverse direction in order to obtain a more distinct switching behaviour. Our results are well compatible with those of the complementary study by Chaleau et al.,¹⁹ who did extensive micromagnetic simulations and investigated the remanent magnetization direction using XMCD experiments.

The authors would like to thank J.-Y. Chaleau for helpful discussions. We gratefully acknowledge funding by the EU FP7 project SE2ND and by the Deutsche Forschungsgemeinschaft via SFB 689, GRK 1570, and Emmy Noether project Hu 1808/1-1.

¹K. Tsukagoshi, B. W. Alphenaar, and H. Ago, "Coherent transport of electron spin in a ferromagnetically contacted carbon nanotube," *Nature* **401**, 572 (1999).

²L. E. Hueso, J. M. Pruneda, V. Ferrari, G. Burnell, J. P. Valdés-Herrera, B. D. Simons, P. B. Littlewood, E. Artacho, A. Fert, and N. D. Mathur, "Transformation of spin information into large electrical signals using carbon nanotubes," *Nature* **445**, 410–3 (2007).

³S. Sahoo, T. Kontos, J. Furer, C. Hoffmann, M. Graber, A. Cotet, and C. Schönenberger, "Electric field control of spin transport," *Nature Physics* **1**, 99–102 (2005).

⁴D. Preusche, S. Schmidmeier, E. Pallecchi, C. Dietrich, A. K. Hüttel, J. Zweck, and C. Strunk, "Characterization of ferromagnetic contacts to carbon nanotubes," *Journal of Applied Physics* **106**, 084314 (2009).

⁵M. Gaass, A. K. Hüttel, K. Kang, I. Weymann, J. von Delft, and C. Strunk, "Universality of the Kondo effect in quantum

- dots with ferromagnetic leads,” *Phys. Rev. Lett.* **107**, 176808 (2011).
- ⁶M. J. Biercuk, S. Garaj, N. Mason, J. M. Chow, and C. M. Marcus, “Gate-defined quantum dots on carbon nanotubes,” *Nano Letters* **5**, 1267–1271 (2005).
- ⁷S. Sahoo, T. Kontos, C. Schönenberger, and C. Sürgers, “Electrical spin injection in multiwall carbon nanotubes with transparent ferromagnetic contacts,” *Applied Physics Letters* **86**, 112109 (2005).
- ⁸C. F. Palma, T. Delattre, P. Morfin, J. M. Berroir, G. Fève, D. C. Glattli, B. Plaçais, A. Cottet, and T. Kontos, “Conserved spin and orbital phase along carbon nanotubes connected with multiple ferromagnetic contacts,” *Phys. Rev. B* **81**, 115414 (2010).
- ⁹F. M. Mueller, A. J. Freeman, J. O. Dimmock, and A. M. Furdyna, “Electronic structure of palladium,” *Phys. Rev. B* **1**, 4617–4635 (1970).
- ¹⁰L. Hodges, R. E. Watson, and H. Ehrenreich, “Renormalized atoms and the band theory of transition metals,” *Phys. Rev. B* **5**, 3953–3971 (1972).
- ¹¹J. C. Ododo, “Percolation concentration and saturation of the Pd moment in ferromagnetic Pd alloys,” *Journal of Physics F: Metal Physics* **13**, 1291–1309 (1983).
- ¹²J. C. Ododo, “The onset of ferromagnetism in transition metal alloys as a cooperative phase transition,” *Journal of Physics F: Metal Physics* **10**, 2515–2534 (1980).
- ¹³G. J. Nieuwenhuys, “Magnetic behaviour of cobalt, iron and manganese dissolved in palladium,” *Advances in Physics* **24**, 515 (1975).
- ¹⁴E. O. Wollan, “Magnetic coupling in the Ni-Pd alloy system,” *Phys. Rev.* **167**, 461–463 (1968).
- ¹⁵J. W. Loram and K. A. Mirza, “Dilute PdNi-a homogeneous magnetic system of fluctuating moments,” *Journal of Physics F: Metal Physics* **15**, 2213–2229 (1985).
- ¹⁶H. Z. Arham, T. S. Khaire, R. Loloe, W. P. Pratt, and N. O. Birge, “Measurement of spin memory lengths in PdNi and PdFe ferromagnetic alloys,” *Phys. Rev. B* **80**, 174515 (2009).
- ¹⁷S. Schmidmeier, *Mikromagnetische Charakterisierung von ferromagnetischen Kontaktelektroden*, diploma thesis, Universität Regensburg (2007).
- ¹⁸J. C. Ododo, “Ferromagnetic correlation lengths in dilute PdFe and PdCo alloys,” *Journal of Physics F: Metal Physics* **15**, 941–951 (1985).
- ¹⁹J.-Y. Chauleau, B. J. McMorran, R. Belkhou, N. Bergeard, T. O. Montes, M. Niño, A. Locatelli, J. Unguris, S. Rohart, J. Miltat, and A. Thiaville, “Magnetization textures in NiPd nanostructures,” *Phys. Rev. B* **84**, 094416 (2011).
- ²⁰M. P. Sarachik, D. R. He, W. Li, M. Levy, and J. S. Brooks, “Magnetic properties of boron-doped silicon,” *Phys. Rev. B* **31**, 1469–1477 (1985).
- ²¹T. McGuire and R. Potter, “Anisotropic magnetoresistance in ferromagnetic 3d alloys,” *IEEE Transactions on Magnetics* **11**, 1018–1038 (1975).
- ²²J. C. Gonzalez-Pons, J. J. Henderson, E. del Barco, and B. Ozyilmaz, “Geometrical control of the magnetization direction in high aspect-ratio pdni ferromagnetic nanoelectrodes,” *Phys. Rev. B* **78**, 012408 (2008).
- ²³S. Chikazumi, *Physics of Ferromagnetism*, 2nd ed. (Oxford, Clarendon Press, 1997).